Evidence of Anisotropic Self-Diffusion of Guest Molecules in Nanoporous Materials of MCM-41 Type

Frank Stallmach,[†] Jörg Kärger,*[,†] Cordula Krause,[†] Markus Jeschke,[‡] and Uwe Oberhagemann[‡]

Contribution from the Fakultät für Physik und Geowissenschaften, Universität Leipzig, Linnéstrasse 5, and Fakultät für Chemie und Mineralogie, Universität Leipzig, Linnéstrasse 4, 04103 Leipzig, Germany

Received March 29, 2000. Revised Manuscript Received July 6, 2000

Abstract: The pore architecture of MCM-41 was investigated by pulsed field gradient nuclear magnetic resonance (PFG NMR) self-diffusion measurements of adsorbed water. Over diffusion length scales which exceed the radius of the one-dimensional channels of the MCM-41 by 2 orders of magnitude but which are smaller than the size of the individual MCM-41 particles, the molecular propagation of the guest molecules was found to be highly anisotropic. The PFG NMR experimental data are best represented by an axisymmetrical diffusion tensor rather than by pure one-dimensional diffusion along the channels. This suggests that the pore walls of the one-dimensional channels are permeable for water or that over the probed diffusion length the channels are disordered and bent. Both interpretations provide information on the pore structure of the nanoporous material which is not available from X-ray diffraction data.

Introduction

Since their introduction into public research in the early 1990s, nanoporous materials of MCM-41 type have received considerable interest among researchers in different areas. In the effort to find new valuable applications for this material, numerous attempts have been made to alter, improve, and characterize their chemical and physical properties as well as their pore structure.[1−4] In contrast, there are only very few and even contradictory reports on the transport properties of molecules hosted in the one-dimensional hexagonally ordered channels of MCM-41.[5−7] There is a substantial deficiency in our knowledge of this material since it is the transport of molecules through the pore network which essentially determines the trapping, the arrangement, the conversion, and the release of molecules that are important for many potential applications.

To our knowledge, macroscopic transport measurements under nonequilibrium conditions[8] are even unreported for MCM-41. Perhaps, due to the low transport resistance which the hexagonally arranged one-dimensional channel system of relatively large diameter (3 nm) of MCM-41 offers to sorbate molecules with small molecular weights, the uptake or tracer exchange rates are much too fast to allow the extraction of transport diffusion coefficients.[8] Moreover, these methods—if they were to be applied to study slower uptake processes of larger molecules such as oligomers or polymers—yield primarily only information on the exchange rate of the adsorbed intraparticle phase with the surrounding gas or liquid phase. Even in such systems, the influence of the internal anisotropic channel structure of the MCM-41 on the intraparticle diffusion remains masked and cannot be extracted from macroscopic methods.

Microscopic self-diffusion measurements under macroscopic equilibrium conditions with the pulsed field gradient (PFG) NMR[8−11] are well established in a large variety of homogeneous and heterogeneous systems. Among the latter are diffusion studies of fluids in porous rocks,[11] nanoporous zeolites,[8,11−13] melts, and solutions of polymers and copolymers,[14,15] as well as fluids confined between self-assembled biological membranes.[10,16] Generally, the solid matrix of the pore wall and/or the repulsive interaction between the fluid phases restrict the self-diffusion of the molecules accommodated in the pore space and the microphases, respectively. It has been demonstrated that PFG NMR may reveal structural information on the pore space or the microphases of such heterogeneous systems via the

[†] Fakultät für Physik und Geowissenschaften.

[‡] Fakultät für Chemie und Mineralogie.

(1) Beck, J. S.; Vartuli, J. C.; Roth, W. J.; Leonowicz, M. E.; Kresge, C. T.; Schmitt, K. D.; Chu, C. T.-W.; Olson, D. H.; Sheppard, E. W.; McCullen, S. B.; Higgins, J. B.; Schlenker, J. L. *J. Am. Chem. Soc.* **1992**, *114*, 10834−10854.

(2) Bounneviot, L., Béland, F., Danumah, C., Giasson, S., Kaliaguine, S., Eds.; *Mesoporous Molecular Sieves 1998*; Studies in Surface Science and Catalysis 117; Elsevier: Amsterdam, 1998.

(3) Janicke, M. T.; Landry, C. C.; Christiansen, S. C.; Kumar, D.; Stuky, G. D.; Chmelka, B. F. *J. Am. Chem. Soc.* **1998**, *120*, 6940−6951.

(4) Springuel-Huet, M.-A.; Sun, K.; Fraissard, J. *Micropor. Mesopor. Mater*. **1999**, *33*, 89−95.

(5) Kärger, J.; Krause, C.; Schäfer, H. *Fortschr.-Ber. VDI, Reihe 3* **1998**, *555* (1), 104−119.

(6) Hansen, E. W.; Courivaud, F.; Karlsson, A.; Kolboe, S.; Stocker, M. *Micropor. Mesopor. Mater.* **1998**, *22*, 309−320. Courivaud, F.; Hansen, E. W.; Karlsson, A.; Kolboe, S.; Stocker, M. *Micropor. Mesopor. Mater.* **2000**, *35/36*, 327−339.

(7) Matthae, F. P.; Basler, W. D.; Lechert H. In *Mesoporous Molecular Sieves 1998*; Bounneviot, L., Béland, F., Danumah, C., Giasson, S., Kaliaguine, S., Eds.; Studies in Surface Science and Catalysis 117; Elsevier: Amsterdam, 1998; pp 301−308.

(8) Kärger J.; Ruthven, D. M. *Diffusion in Zeolites and other Microporous Solids*; Wiley-Interscience: New York, 1992.

(9) Stejskal, E. O.; Tanner, J. E. *J. Chem. Phys*. **1965**, *42*, 288−292.

(10) Callaghan, P. T. *Principles of Nuclear Magnetic Resonance Microscopy*; Clarendon Press: Oxford, 1991.

(11) Stallmach, F.; Kärger, J. *Adsorption* **1999**, 5, 117−133.

(12) Bär, N.-K.; Kärger, J.; Pfeifer, H.; Schäfer, H.; Schmitz, W. *Micropor. Mesopor. Mater*. **1998**, *22*, 289−295.

(13) Heink, W.; Kärger, J.; Pfeifer, H.; Stallmach, F. *J. Am. Chem. Soc*. **1990**, *112*, 2175−2178.

(14) Fleischer, G.; Fujara, F. *NMR* **1994**, *30*, 161−207.

(15) Rittig, F.; Kärger, J.; Papadakis, Ch. M.; Fleischer, G.; Stepanek, P.; Almdal, K. *Phys. Chem. Chem. Phys.* **1999**, *1*, 3923−3931.

(16) Waldeck, A. R.; Kuchel, P. W.; Lennon, A. J.; Chapman, B. E. *Prog. Nucl. Magn. Reson. Spectrosc.* **1997**, *30*, 39−68.

10.1021/ja001106x CCC: $19.00
Published on Web 09/06/2000

observation of the restricted self-diffusion.[9−11] Moreover, if the heterogeneous system is formed by anisotropic structure elements, the self-diffusion tensor, which describes the resulting anisotropic self-diffusion process of the fluid molecules, may be obtained directly from the typical pattern of the PFG NMR spin−echo attenuation.[10−12,15] Depending on the system studied and the experimental equipment available, the diffusion length scales probed by this technique reach from 0.1 μm up to a few hundred micrometers.

These remarkable features of PFG NMR were recently recognized by researchers interested in transport phenomena in nanoporous materials of MCM-41 type. Among the very few papers published so far, there are a few consistent results but also some contradictory results. For water, cyclohexane, neopentane, *n*-pentane, *n*-dodecane,[7] and *n*-hexadecane,[5,17] the averaged self-diffusion coefficient (exactly the trace of the self-diffusion tensor) of fluid molecules in the MCM-41 was found to be reduced by about 1−2 orders of magnitude compared to the bulk diffusivity of the same fluid. In contrast, *n*-hexane[6] shows only a slight reduction, while benzene[18] even shows an enhancement of its self-diffusivity in the nanoporous host system. In refs 6 and 7, the authors did not take into account that the anisotropic pore system of the MCM-41 should lead to an anisotropic self-diffusion with distinct deviations from the monoexponential spin−echo attenuation usually observed in the case of self-diffusion in isotropic systems. In the PFG NMR measurements with *n*-hexane[6] and *n*-hexadecane,[5,17] deviations from a monoexponential spin−echo attenuation are reported. However, in ref 6 the observed patterns are analyzed in terms of isotropic diffusion in two-region systems consisting of an adsorbed phase (intraparticle) and a gas (interparticle) phase with exchange between them using the model of the NMR tracer desorption technique.[8] Only in our previous work with *n*-hexadecane was the possible influence of the anisotropic pore system of the MCM-41 on the self-diffusion considered.[5,17] It was demonstrated that the observed spin−echo attenuations were consistent with an axisymmetrical self-diffusion tensor. The axial and radial elements of this tensor were assigned to the fast self-diffusion parallel (D_{par}) and a much smaller but finite self-diffusion perpendicular (D_{perp}) to the one-dimensional channels, respectively. This interpretation led us to the hypothesis that the silica matrix of the one-dimensional channels must be permeable or disordered over the probed diffusion length. However, at that time we were not able to exclude effects of interparticle and gas diffusion, as they were obviously observed in ref 6.

This paper presents the first data on intraparticle self-diffusion of adsorbed molecules in MCM-41 which are clearly not affected by interparticle diffusion between neighboring particles through the void space of the particle bed. We will show that (i) the intraparticle self-diffusion of water in MCM-41 is, in fact, anisotropic and best described by an axisymmetrical self-diffusion tensor, that (ii) the observed anisotropy for long diffusion lengths is consistent with the morphology of the individual MCM-41 particles and confirms the suggested preferential orientation of the one-dimensional channels inside the individual particles, and finally that (iii) the anisotropy at short diffusion lengths evidences a permeable or disordered silica matrix of the MCM-41 which is not detectable by other methods of structural analysis.

(17) Kärger, J.; Krause, C.; Schäfer, H. *GIT Spez. Chromatigr.* **1997**, *1*, 26−28.

(18) Stallmach, F.; Gräser, A.; Kärger, J.; Krause, C.; Jeschke, M.; Oberhagemann, U., Spange, S. *Micropor. Mesopor. Mater.*, in press.

Theoretical Section

Pulsed Field Gradient NMR. Pulsed field gradient NMR self-diffusion measurements are based on NMR pulse sequences which generate a primary or stimulated spin−echo of the magnetization of the resonant nuclei. By appropriate addition of pulsed magnetic field gradients of duration δ, intensity g, and distance Δ (observation time) in the defocusing and refocusing period of the NMR pulse sequence, the observed spin−echo becomes sensitive to the translational motion of the molecules which carry the nuclear spin under investigation. In the case of a stochastic transport process under macroscopic equilibrium conditions such as the thermally excited Brownian molecular motion (self-diffusion), the spin−echo intensity $M(\delta g,\Delta)$ is attenuated. Assuming that the pulsed field gradient is applied along the z-axis of the laboratory frame of reference, the attenuation factor is given by[8−11]

$$\Psi(\delta g,\Delta) = \frac{M(\delta g,\Delta)}{M(\delta g = 0,\Delta)} = \exp\left[-(\gamma\delta g)^2 \frac{1}{2}\langle z^2(\Delta)\rangle\right] \quad (1)$$

where $\langle z^2(\Delta)\rangle$ denotes the mean square displacement of the diffusing molecules in the direction of the pulsed field gradient during the observation time. γ is the gyromagnetic ratio of the observed type of nuclei (^{1}H, $\gamma = 2.67 \times 10^8$ (T s)$^{-1}$). For any diffusion process one may define an apparent time-dependent self-diffusion coefficient $D_z(\Delta)$ along the z-direction by

$$\langle z^2(\Delta)\rangle = 2D_z(\Delta)\Delta \quad (2)$$

where for normal (unrestricted) self-diffusion D_z is independent of observation time and eq 2 becomes the well-known Einstein relation. With eq 2, the time-dependent self-diffusion coefficient or the mean square displacement can be used to describe the self-diffusion process. According to eqs 1 and 2, both values may be measured by PFG NMR from the slope of the semilogarithmic plot of the spin−echo attenuation as a function of the square of the applied pulsed field gradient strength ($\ln \Psi$ vs $(\gamma g\delta)^2$).

It is an inherent principle of PFG NMR that the displacement of molecules is monitored in one spatial dimension which is defined by the direction of the pulsed field gradient. Since, however, self-diffusion processes occur in most systems in three-dimensional space, one has to consider that the total mean square displacement $\langle r^2(\Delta)\rangle$ is given by the sum of the mean square displacements in the three orthogonal directions:

$$\langle r^2(\Delta)\rangle = \langle x^2(\Delta)\rangle + \langle y^2(\Delta)\rangle + \langle z^2(\Delta)\rangle = 6D(\Delta)\Delta \quad (3)$$

Equation 3 defines the three-dimensional self-diffusion coefficient $D(\Delta)$ in a way similar to that in eq 2. It is related to its three orthogonal components by

$$D = \frac{1}{3}(D_x + D_y + D_z) \quad (4)$$

In the case of diffusion in isotropic systems, the self-diffusion coefficients in the three orthogonal directions are the same ($D_x = D_y = D_z$). Thus, it holds that $D = D_z$, which means that $D(\Delta)$ can be measured directly by PFG NMR.

Model for Anisotropic Self-Diffusion in MCM-41. If the system studied is anisotropic, then the displacement of the molecules on the direction of the pulsed field gradient and hence the observed spin−echo attenuation depends on the orientation of the system with respect to the pulsed field gradient. Molecules adsorbed in MCM-41 are subjected to the following micrody-

namic situation, which is caused by the anisotropic pore structure of MCM-41 consisting of hexagonally arranged channels: The appearance of higher-order peaks in the small-angle X-ray diffraction patterns requires that there exists a long-range order of the channels; i.e., the channels form domains, each of them characterized by a certain direction of the channel axis.[19] The domain size must clearly exceed the diameter of the channels (3 nm). Therefore, we will refer to these regions of ordered hexagonally arranged channels as "nanoscopic domains". Over the extension of such a nanoscopic domain, the MCM-41 has an axisymmetrical pore structure. Molecular transport of sorbed species through the pore system preferentially occurs along the channel axis. Possible transport processes perpendicular to this direction would require the molecules to pass through the silica walls or to jump from channel to channel at the end of the channels. Obviously, the transport resistance for a molecule moving along the channel axis is much smaller than that for a molecule traveling from channel to channel. Therefore, for root-mean-square (rms) displacements which are smaller than the size of the nanoscopic domain, the self-diffusion coefficient parallel to the channel direction (D_{par}) is expected to be much larger than the self-diffusion coefficient perpendicular to it (D_{perp}). On such length scales, it is justified to assume that an axisymmetrical tensor **D** describes the self-diffusion inside the pore system:

$$\mathbf{D} = \begin{pmatrix} D_{par} & 0 & 0 \\ 0 & D_{perp} & 0 \\ 0 & 0 & D_{perp} \end{pmatrix}, \quad D_{par} > D_{perp} \geq 0 \qquad (5)$$

If such an anisotropic self-diffusion process is studied by PFG NMR, it has to be considered that the observed mean square displacement depends on the orientation of the channels with respect to the pulsed field gradients (z-direction). If Θ denotes the polar angle of this orientation, the actually measured mean square displacement is[10,20]

$$\langle z^2(\Delta)\rangle = 2D_{par}(\Delta)\Delta \cos^2\Theta + 2D_{perp}(\Delta)\Delta \sin^2\Theta \qquad (6)$$

According to eq 1, this means that the spin−echo attenuation depends on the orientation. Since an individual MCM-41 particle may consist of several nanoscopic domains of such hexagonally arranged channels, and since in an NMR sample these particles are randomly oriented, the actual spin−echo attenuation is found by the powder average of eqs 1 and 6 with respect to Θ, which yields[10,20]

$$\Psi(\delta g,\Delta) = \frac{1}{2}\int_0^{\pi} \exp\{-(\gamma\delta g)^2\Delta(D_{par}\cos^2\Theta + D_{perp}\sin^2\Theta)\}\sin\Theta\, d\Theta \qquad (7)$$

In contrast to the case of normal self-diffusion presented by eq 1, eq 7 is not an exponentially decaying function with respect to the square of the applied pulsed field gradient strength. Thus, for PFG NMR measurements with molecules adsorbed in the nanoporous anisotropic channel system of the MCM-41, the observation of a nonexponential spin−echo attenuation is expected. If the spin−echo attenuation follows the typical pattern presented by eq 7, the hypothesis of an axisymmetrical self-diffusion tensor may be confirmed experimentally, and the two components of the tensor may be determined. Moreover, additional information on the influence of the pore structure on the molecular transport can be obtained by analyzing the two elements of the self-diffusion tensor.

The integral in eq 7 cannot be solved analytically. For the calculation of theoretical spin−echo attenuations as well as for fitting of experimental results, it must be approximated by a sum. For our data analysis, a sum consisting of 84 terms equally spaced between $0 \leq \Theta \leq \pi$ was used. This number was found to be sufficient for the approximation of the integral.

Experimental Section

Description of the Si-MCM-41 Material. Si-MCM-41 was synthesized in a way similar to that described in ref 21. The material shows seven peaks in the X-ray diffraction, indicating highly ordered hexagonally arranged channels. The individual particles exhibit preferentially rodlike shapes with a length of $l = 4.0 \pm 0.5$ μm and a diameter of $d = 1.0 \pm 0.2$ μm. Details of the syntheses as well as results of the characterization of the material by small-angle X-ray diffraction and SEM are given in the Supporting Information.

Preparation of NMR Samples. For the PFG NMR measurements, about 60 mg of the calcined Si-MCM-41 powder was filled into an NMR sample tube of 7.5 mm outer diameter. The powder was mixed with about 0.5 mL of distilled water by stirring with a glass rod. To remove remaining air bubbles from the suspension, the sample was evacuated up to the vapor pressure of water and exposed subsequently to ambient pressure conditions. Afterward, the sample tube was sealed tightly and stored for at least 48 h at room temperature to allow for the water to diffuse into the nanopores of the MCM-41.

Prior to NMR measurements, the samples were stirred again in order to ensure a homogeneous distribution of the MCM-41 particles in the suspension. The samples were always introduced at room temperature into the probe of the NMR spectrometer. PFG NMR diffusion measurements as described below were performed in the temperature range from 269 to 235 K, where the interparticle water of the suspension is frozen to ice. As a consequence of the dramatically reduced transverse relaxation time, the frozen water no longer contributes to the observed NMR signal. The intraparticle water in the nanopores of the MCM-41, however, which freezes at a much lower temperature due to the Kelvin law, still yields a sufficient signal-to-noise ratio of the NMR signal to permit the observation of the spin−echo (see also the Results section).

Details of the PFG NMR Measurements. PFG NMR self-diffusion measurements were carried out by using the home-built NMR spectrometer FEGRIS 400 operating at 400 MHz ^{1}H resonance frequency.[22] The stimulated spin−echo pulse sequence which consists of three 90° rf pulses was used to generate the NMR signal. The delay between the first and the second rf pulses (τ_1) was fixed to 2 ms, which ensured a sufficient T_2 weighting of the observed stimulated spin−echo to exclude signal contributions from the frozen interparticle water phase. Rectangular-shaped pulsed field gradients of a duration δ of up to 1.2 ms were applied immediately after the first and the third rf pulse. The dependence of the self-diffusion on observation time Δ was studied in an interval from 5 to 60 ms, which was achieved by varying the delay between the second and the third rf pulse (τ_2). The spin−echo attenuation was monitored for each observation time by increasing the intensity g of the pulsed field gradients in 16 steps from zero up to 22 T/m.

Results

Exclusion of Interparticle Diffusion by Freezing of the Interparticle Phase. At room temperature, a very intense stimulated spin−echo was observed which originated from both the inter- and the intraparticle water phase. Upon cooling of the sample to 269 K (−4 °C), the interparticle water phase freezes to ice. Simultaneously, the intensity of the stimulated

(19) Chen, C.-Y.; Xiao, S.-Q.; Davis, M. E. *Micropor. Mater.* **1995**, *4*, 1−20.
(20) Kärger, J.; Pfeifer, H.; Heink, W. *Adv. Magn. Reson.* **1988**, *12*, 1−89.
(21) Oberhagemann, U.; Jeschke, M.; Papp, H. *Micropor. Mesopor. Mater.* **1999**, *33*, 165−172.
(22) Kärger, J.; Bär, N.-K.; Heink, W.; Pfeifer, H.; Seiffert, G. *Z. Naturforsch.* **1995**, *50a*, 186−190.

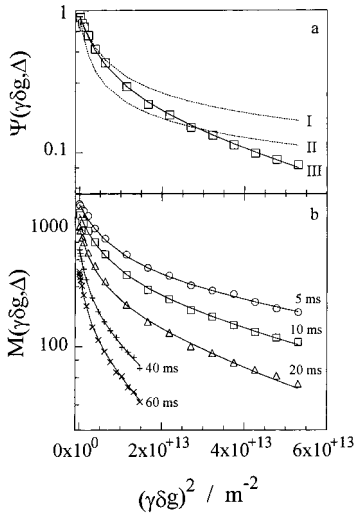

Figure 1. Example of ^{1}H PFG NMR diffusion measurements of water in MCM-41. (a) Comparison of the experimentally observed spin−echo attenuation at 10 ms observation time (□) with theoretically expected curves for three axisymmetrical self-diffusion tensors (curves I−III). Curves I and II represent pure one-dimensional diffusion along straight channels and are calculated from eq 7 with vanishing perpendicular component of the self-diffusivity. Only curve III, with a finite perpendicular self-diffusivity, leads to a good agreement with the experimental data. (b) Dependence of the spin−echo intensity on the pulsed field gradient strength and on the observation time (5−60 ms) for the same sample. The lines represent the fits of the model of an axisymmetrical diffusion tensor with finite perpendicular self-diffusivity (eq 7) to the experimental data. All measurements were performed at 263 K.

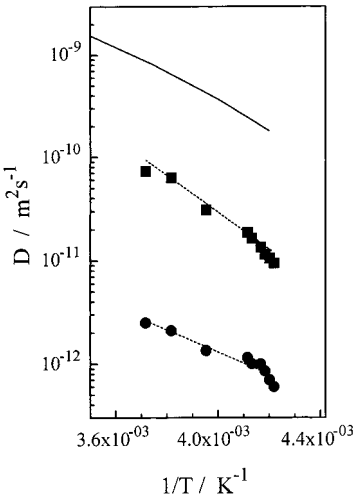

Figure 2. Dependence of the parallel (■) and perpendicular (●) components of the axisymmetrical self-diffusion tensor on the inverse temperature for water in MCM-41 as measured at 10 ms observation time with PFG NMR. The dotted lines may be used as a guide for the eyes. For comparison, the full line represents the self-diffusion coefficients of supercooled bulk liquid water as obtained from Figure 1 in ref 23.

spin−echo drops by 2−3 orders of magnitude. Because of the very short transverse relaxation time of the ^{1}H nuclei of ice, the frozen interparticle water, obviously, does not contribute to the stimulated spin−echo generated with a τ_1 delay of 2 ms in the rf pulse sequence.

At short observation times and at temperatures above 237 K, the remaining signal-to-noise ratio of the stimulated spin−echo was still always larger than 100. Since earlier NMR relaxation measurements of water in MCM-41[7] showed that the transverse (T_2) relaxation times are in the range from 3 to 1 ms and the longitudinal (T_1) relaxation times are from about 70 to 30 ms (depending, e.g., on pore size and temperature), the remaining NMR signal was assigned to the water inside the nanopores. Below 237 K, it was not possible to observe a stimulated spin−echo under the experimental conditions described above. This is also in agreement with the reported rapid drop of transverse relaxation times at temperatures below 240 K,[7] which is caused by the loss of the motional averaging of the dipole−dipole interaction of the ^{1}H nuclei at such low temperatures at the pore walls. Thus, in the temperature range from 269 to 237 K, only intraparticle water molecules contribute to the observed NMR signal.

Data Analysis of PFG NMR Measurements. The measured spin−echo attenuations at all temperatures and observation times did not decay monoexponentially with the square of the pulsed field gradient strength. As an example, Figure 1a presents the spin−echo attenuation obtained at 263 K and 10 ms observation time. The nonexponential spin−echo decay excludes the interpretation in terms of isotropic self-diffusion (eq 1) inside the MCM-41 particles. For pure one-dimensional anisotropic diffusion in straight channels, spin−echo attenuations according to curves I and II (Figure 1a) would be expected. They were calculated from eq 7 with the perpendicular self-diffusion coefficient set equal to zero ($D_{perp} = 0$; curve I, $D_{par} = 5.7 \times 10^{-11}$ m^2 s^{-1}; curve II, $D_{par} = 1.4 \times 10^{-10}$ m^2 s^{-1}). Only the anisotropic self-diffusion model, which assumes an axisymmetrical self-diffusion tensor with finite self-diffusion coefficients parallel *and* perpendicular to the channel axis (curve III, $D_{par} = 5.7 \times 10^{-11}$ m^2 s^{-1} and $D_{perp} = 1.6 \times 10^{-12}$ m^2 s^{-1}), yields a good agreement with the observed spin−echo attenuation.

As demonstrated in Figure 1b, the same model of anisotropic self-diffusion was sufficient to explain the dependence of the spin−echo attenuations on the observation time. The experimentally observed spin−echo intensities (not the attenuations) for the same sample as in Figure 1a and the fits according to eq 7 are shown. The decay of the intensity at $(\gamma\delta g)^2 = 0$ with increasing observation time is governed by the longitudinal relaxation process during the τ_2 delay in the pulse sequence. The T_1 relaxation time determined from this decay was found to be 44 ± 8 ms, which agrees well with the previously published values for water adsorbed in MCM-41.[7] This provides further evidence that the water inside the nanopores is observed under the chosen experimental conditions.

Diffusivities Obtained from the Axisymmetrical Self-Diffusion Model. The model of an axisymmetrical self-diffusion of water in MCM-41 was found to fit the spin−echo attenuations over the total range of temperatures and observation times considered in the experiments. It yielded the parallel and the perpendicular components of the self-diffusion tensor which may be used to evaluate the transport of water inside the MCM-41 particles. The temperature dependence of these components as obtained from the measurements at 10 ms observation time is given in an Arrhenius plot in Figure 2. For comparison, the temperature dependence of the self-diffusion of supercooled water as reported in ref 23 is also included. The parallel component of the water self-diffusion is found to be reduced by approximately 1 order of magnitude compared with that of bulk water at the same temperature. The perpendicular component is even smaller. The anisotropy factor, which may be defined as the ratio between the perpendicular and the parallel

(23) Weingärtner, H. *Z. Phys. Chem. Neue Folge* **1982**, *132*, 129−149.

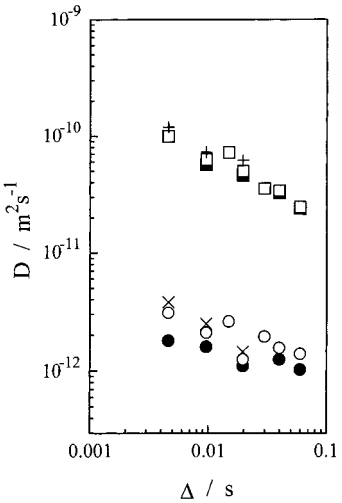

Figure 3. Dependence of the parallel (■, □, +) and perpendicular (●, ○, ×) components of the axisymmetrical self-diffusion tensor on the observation time for water in MCM-41 at 263 K (squares and circles, two samples) and 269 K (crosses, only one sample).

components of the self-diffusion tensor,

$$\eta = \frac{D_{\text{perp}}}{D_{\text{par}}} \tag{8}$$

averaged over the investigated temperature range, is about 0.05 ± 0.02.

Figure 3 shows the dependences of the parallel and the perpendicular components of the self-diffusion tensor at 269 and 263 K on the observation time for two samples of the same MCM-41 which differ only in the amount of interparticle water. Within the experimental error, the data for the two samples are consistent and yield the same anisotropy factor, $\eta = 0.034 \pm 0.006$. The decrease of the self-diffusion coefficients with increasing observation time indicates the existence of transport resistances on the diffusion path. Their nature will be discussed below.

Discussion

The observed nonexponentially decaying spin−echo attenuations allow only the conclusion that the monitored transport process is anisotropic and best described by an axisymmetrical self-diffusion tensor. Since the interparticle space is blocked by the frozen water, the observed transport process is restricted to the intraparticle space. Therefore, the presented data must be considered as the first experimental evidence for anisotropic self-diffusion within MCM-41 particles which are not affected by any contribution from interparticle diffusion.

The origin of the anisotropy of the self-diffusion must be sought in the morphology of the MCM-41 material. There are two possible reasons for the observed behavior, viz., (i) the "microscopic" anisotropy of the individual particles itself as observed by SEM and light microscopy and (ii) the inherent "nanoscopic" anisotropy of the axisymmetrical pore structure inside the domains of the hexagonally arranged channels forming an individual particle. Using Einstein's relation (eq 2), the observed time dependence of the self-diffusivities (Figure 3) may be transformed into the corresponding time dependence of mean square displacements. Figure 4 shows these data for the parallel and perpendicular components of the self-diffusion. Both time dependences reflect some kind of restricted self-diffusion, since the mean square displacements do not increase

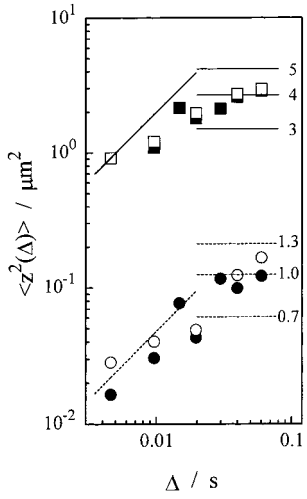

Figure 4. Dependence of the parallel (■, □) and perpendicular (●, ○) components of the mean square displacement on the observation time for water in two MCM-41 samples at 263 K. The mean square displacements were calculated via eq 2 from the components of the axisymmetrical self-diffusion tensor plotted in Figure 3. The horizontal lines indicate the limiting values for the axial (full lines) and radial (dotted lines) components of the mean square displacements for restricted diffusion in cylindrical rods which were determined via eq 9. The lengths l and diameters d of the rods are given in units of micrometers on the lines. The oblique lines (45°), which are plotted for short observation times only, represent the calculated time dependences of the mean square displacements for unrestricted (free) diffusion with $D_{\text{par}} = 1.0 \times 10^{-10}$ m^2 s^{-1} (full line) and $D_{\text{perp}} = 2.0 \times 10^{-12}$ m^2 s^{-1} (dotted line), respectively.

linearly with the observation time. The origin of the restriction becomes clear if one compares the mean square displacements observed with the limiting values expected for restricted self-diffusion inside a cylinder of length l and diameter d at infinite observation times. These limiting values may be calculated to be[10,11,20]

$$\langle z^2(\Delta \rightarrow \infty)\rangle = \begin{cases} \frac{1}{6}l^2 \\ \frac{1}{8}d^2 \end{cases} \tag{9}$$

The horizontal lines in Figure 4 indicate these limiting values for $l = 3-5$ μm and $d = 0.70-1.3$ μm. Obviously, the mean square displacements at 60 ms observation time are consistent with restricted diffusion in a cylinder of about 4 μm length and about 1.0−1.3 μm diameter. Since these values agree satisfactorily with the length and diameter of the rodlike MCM-41 particles determined by SEM, it must be the "shape" anisotropy of the particles which determines the diffusion anisotropy at long observation times. For restricted diffusion in a rodlike particle, according to eq 9 the anisotropy factor η_s is given by the ratio of the limiting mean square displacements:

$$\eta_s = \frac{6d^2}{8l^2} \tag{10}$$

Application of eq 10 to the MCM-41 particles used yields a value of $\eta_s = 0.047 \pm 0.030$. From the mean square displacements at 60 ms, an experimental anisotropy factor of $\eta(60\text{ ms}) = 0.05 \pm 0.02$ is obtained. Although the experimental uncertainties in both anisotropy factors, which are caused by the uncertainties in the measurements of the particle size and the mean square displacement, are quite large, the agreement between both values may be taken as a consistency check of

the statement that "shape" anisotropy controls the observed diffusion anisotropy at long observation times.

With decreasing observation times, the anisotropy factor shows a tendency to decrease. This means that with decreasing observation times the reduction in the confinement by the external particle shape is more pronounced for molecular transport perpendicular to the particle axes than for that parallel to them. One has to conclude, therefore, that the channels are preferentially oriented along the longitudinal extensions of the particles and that the rate of molecular transport perpendicular to this direction is still smaller than that indicated by the anisotropy factor of restricted diffusion (eq 10).

One of our goals in carrying out PFG NMR diffusion measurements is to derive information about the nanoscopic diffusion anisotropy caused by the pore architecture. This is possible in a direct way only if the observed rms displacements of the adsorbed molecules are smaller than the size of the nanoscopic domains of the hexagonally arranged channels. The smallest rms displacements of the water molecules observed in this work are about 1 μm for the parallel component and about 0.15 μm for the perpendicular component of the self-diffusion tensor. To our knowledge, there does not exist an experimentally verified estimate for the size of the nanoscopic domains. Combining the conclusions of the presented diffusion data (particularly concerning the existence of a finite perpendicular component of the diffusion tensor), the microscopically determined particle size and the small-angle X-ray structure data lead to fundamental consequences for the real structure of the channels of the MCM-41:

(1) If we assume that the size of the domains is the same as the particle size, i.e., one particle consists of one domain only, it follows that the silica walls of the channels must be permeable for water: Nonpermeable silica walls would restrict the perpendicular self-diffusion to the diameter of the channels (3 nm), which would limit the rms displacements in this direction according to eq 9 to about 1 nm. However, the observed perpendicular rms displacements exceed this value by at least 2 orders of magnitude, which under the above assumption is possible only if the water molecules may penetrate the wall.

(2) If the channel walls are impenetrable, individual particles must consist of more than one domain (i.e., more than one orientation of the channels with respect to the axis of the rod) in order to achieve the observed perpendicular rms displacements. The size of the domains must be on the order of or even much smaller than the smallest rms displacements observed. Thus, a water molecule traveling along the channel has the opportunity to change the direction of its translational motion at the domain border, which might occur by (i) hopping from one individual channel to another one (in the same or a neighboring domain) or by (ii) continuing diffusion in one channel which is slightly bent into another direction. Both processes are sufficient to explain the observed perpendicular self-diffusion. There is no need for permeability of the silica walls. However, both processes require that the particles consist of more than one domain.

Arguments for assumption (1) are the postulated inherent roughness of the surface of the silica walls[4,24,25] as well as heterogeneities and the disorder in the wall structure[25,26] in MCM-41 discussed in recent publications. They suggest the hypothesis that there might also exist holes in the relatively thin walls which would allow small molecules such as water to pass from one channel into a neighboring one, leading finally to permeable walls. Assumption (2) is supported by SEM images which show that the MCM-41 particles used are not always straight rods. This means that, in fact, domains with different orientations of the hexagonally arranged channels form an individual particle, which may lead immediately to the observed perpendicular self-diffusion components. Unfortunately, there is no opportunity to distinguish between these two explanations for the observed perpendicular self-diffusion components on the basis of our experimental results or further literature data of MCM-41. This would require additional knowledge on the morphology of MCM-41 which is not available so far.

The observed similarities in the temperature dependences (activation energy) of the water self-diffusion in the MCM-41 for both the parallel and the perpendicular components as well as in the bulk (Figure 2) suggest that the self-diffusion in the bulk and inside the nanopores follows the same thermodynamic processes. This includes also slight deviations in the linearity of the Arrhenius plots which also exist for bulk water.[23] Obviously, the nanopores of 3 nm diameter do not represent an additional energetic barrier for the water self-diffusion. Consequently, the reduced overall diffusivity must be caused by steric obstructions which the water molecules experience on their diffusion path through the nanopores. The distance between these obstructions must be smaller than the observed diffusion paths, since otherwise D_{par} should be expected to approach the diffusivity of the bulk water for the shortest observation time.

Conclusion

Intraparticle self-diffusion of water sorbed in MCM-41 was studied by PFG NMR. The experimental results clearly evidence the anisotropy of the intraparticle self-diffusion. The components of the obtained axisymmetrical self-diffusion tensor are assigned to diffusion parallel and perpendicular to the channel axis of the hexagonally arranged channel system.

A finite value of the perpendicular self-diffusivity over length scales, which exceed the radius of the one-dimensional channels of the MCM-41 by 2 orders of magnitude, requires the existence of disorder in the channel architecture inside the individual particles. If permeable silica walls are responsible for the observed perpendicular self-diffusion, some kind of "windows" or "microporosity" interconnecting the straight channels has to exist. If such a permeability can be excluded, the individual MCM-41 particles must consist of domains of different channel orientations, as is the case for bent channels or particles formed by an ensemble of channel domains. Both routes of interpretation of the PFG NMR results provide additional information on the pore architecture of this nanoporous material which is not available from X-ray diffraction data.

Acknowledgment. Financial support by the Deutsche Forschungsgemeinschaft (Schwerpunktprogramm "Nanostrukturierte Wirt/Gast-Systeme" and SFB 294, "Moleküle in Wechselwirkung mit Grenzflächen") is gratefully acknowledged.

Supporting Information Available: Scheme for synthesis of Si-MCM-41 under high-pressure conditions and the characterization of the obtained nanoporous material by X-ray diffraction and SEM (PDF). This material is available free of charge via the Internet at http://pubs.acs.org.

JA001106X

(24) Sonwane, C. G.; Bhatia, S. K.; Calos, N. J. *Langmuir* **1999**, *15*, 4603−4612.
(25) Sayari, A. *Langmuir* **1999**, *15*, 5683−5688.
(26) Pophal, C.; Fuess, H. *Micropor. Mesopor. Mater.* **1999**, *33*, 242−247.